

**IDENTIFICATION OF COVID-19, PNEUMONIA, LUNG CANCER & TB FROM
CHEST X-RAY IMAGES: A DEEP TRANSFER LEARNING APPROACH**

BY

GOURAB DATTA

ID: 191-15-2384

AND

MD. ZIA UDDIN

ID: 191-15-2543

This Report Presented in Partial Fulfillment of the Requirements for the Degree of
Bachelor of Science in Computer Science and Engineering

Supervised By

MD. SABAB ZULFIKER

Lecturer (Senior Scale)

Department of Computer Science and Engineering
Daffodil International University

Co-Supervised By

MD. MAHFUJUR RAHMAN

Lecturer (Senior Scale)

Department of Computer Science and Engineering
Daffodil International University



DAFFODIL INTERNATIONAL UNIVERSITY

DHAKA, BANGLADESH

JANUARY 2023

APPROVAL

This Project titled “IDENTIFICATION OF COVID-19, LUNG CANCER, PNEUMONIA, AND TB FROM CHEST X-RAY IMAGES: A DEEP TRANSFER LEARNING APPROACH”, submitted by Gourab Datta, ID No: 191-15-2384, Md Zia Uddin, ID No: 191-15-2543 to the Department of Computer Science and Engineering, Daffodil International University has been accepted as satisfactory for the partial fulfilment of the requirements for the degree of B.Sc. in Computer Science and Engineering and approved as to its style and contents. The presentation has been held on 25-01-23.

BOARD OF EXAMINERS

Chairman

Dr. Touhid Bhuiyan

Professor and Head

Department of Computer Science and Engineering
Faculty of Science & Information Technology
Daffodil International University

Internal Examiner

Shouh

Dr. Md. Atiqur Rahman

Associate Professor

Department of Computer Science and Engineering
Faculty of Science & Information Technology
Daffodil International University

Internal Examiner

Shayla Sharmin
Shayla Sharmin 25.1.23

Senior Lecturer

Department of Computer Science and Engineering
Faculty of Science & Information Technology
Daffodil International University

External Examiner

Farid
25-01-23

Dr. Dewan Md Farid

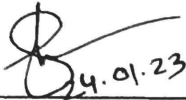
Professor

Department of Computer Science and Engineering
United International University

DECLARATION

We hereby declare that this project has been done by us under the supervision of **Md. Sabab Zulfiker, Lecturer (Senior Scale), Department of CSE Daffodil International University**. We also declare that neither this project nor any part of this project has been submitted elsewhere for the award of any degree or diploma.

Supervised by:



24.01.23

Md. Sabab Zulfiker
Lecturer (Senior Scale)
Department of CSE
Daffodil International University

Co-Supervised by:

Md. Mahfujur Rahman
Lecturer (Senior Scale)
Department of CSE
Daffodil International University

Submitted by:



Gourab Datta
ID: 191-15-2384
Department of CSE
Daffodil International University



Md. Zia Uddin
ID: 191-15-2543
Department of CSE
Daffodil International University

ACKNOWLEDGEMENT

First, we express our heartiest thanks and gratefulness to almighty God for His divine blessing made us possible to complete the final year project/internship successfully.

We really grateful and wish our profound indebtedness to **Supervisor Md. Sabab Zulfiker, Lecturer (Senior Scale)**, Department of CSE, Daffodil International University, Dhaka. Deep Knowledge & keen interest of our supervisor in the field of “**Deep Convolution Neural Networks**” to carry out this project. His endless patience, scholarly guidance, continual encouragement, constant and energetic supervision, constructive criticism, valuable advice, reading many inferior drafts and correcting them at all stages have made it possible to complete this project.

We would like to express our heartiest gratitude to Md. Sabab Zulfiker, Md. Mahfujur Rahman, and Dr. Touhid Bhuiyan, Head, Department of Computer Science and Engineering, for his kind help to finish our project and also to other faculty members and the staff of the CSE department of Daffodil International University.

We would like to thank our entire course-mates at Daffodil International University, who took part in this discussion while completing the coursework.

Finally, we must acknowledge with due respect the constant support and patients of our parents.

ABSTRACT

Due to Lung Cancer, Pneumonia, Tuberculosis, and COVID-19, which have a very terrible effect on the body, the patient may die and COVID-19 spreads very easily. It is possible to get rid of these diseases if they are detected as soon as possible. With the help of Artificial Intelligence detection of these types of diseases will be very easy and quick. AI can detect these types of diseases automatically and accurately. The use of this type of automated and accurate process in the medical sciences will be very beneficial in the modern era of science and technology. In our study, we use Deep Learning to detect 4 major types of lung diseases including- Lung Cancer, Pneumonia, Tuberculosis and COVID-19. We have used a total of 7,255 patients' chest X-ray images as the dataset. The dataset is divided into 5 classes including- Pneumonia, COVID-19, Tuberculosis, Lung Cancer and Normal. Classify those diseases we used 6 very popular deep transfer learning models including- ResNet50, VGG16, EfficientNet, VGG19, MobileNet, and InceptionV3. Among them, the best accuracy has been gained in ResNet50. Based on chest X-ray images, we obtained a test accuracy of 97.65% and a training accuracy of 99.67% from ResNet50. We also obtained trained accuracy of 97.44%, 97.23%, 96.82%, 94.33% and 90.73% respectively in VGG16, EfficientNet, VGG19, MobileNet and Inception-V3.

TABLE OF CONTENTS

| CONTENTS | PAGE |
|------------------------------------|---------------|
| Board of examiners | i |
| Declaration | ii |
| Acknowledgement | iii |
| Abstract | iv |
| CHAPTER | |
| CHAPTER 1: INTRODUCTION | 1 - 3 |
| 1.1 Introduction | 1 |
| 1.2 Motivation | 2 |
| 1.3 Research Objective | 2 |
| 1.4 Rationale of the study | 3 |
| 1.5 Organization of the Report | 3 |
| CHAPTER 2: BACKGROUND STUDY | 4 - 7 |
| 2.1 Related Works | 4 |
| 2.2 Research Summary | 4 |
| 2.3 Scope & Challenges | 7 |
| CHAPTER 3: METHODOLOGY | 8 - 19 |
| 3.1 Introduction | 8 |
| 3.2 Workflow | 8 |
| 3.3 Data Collection | 9 |
| 3.4 Preprocessing of Data | 10 |
| 3.5 Data Splitting | 10 |

| | |
|---|--------------|
| 3.6 Deep Transfer Learning Architecture | 11 |
| 3.6.1 Convolutional Layer | 12 |
| 3.6.2 Pooling Layer | 13 |
| 3.6.3 Fully Connected Layer | 14 |
| 3.7 Pre-Trained Models | 15 |
| 3.7.1 ResNet50 | 16 |
| 3.7.2 EfficientNet | 16 |
| 3.7.3 VGG-16 | 17 |
| 3.7.4 VGG-19 | 17 |
| 3.7.5 Inception-V3 | 18 |
| 3.7.6 MobileNet | 18 |
| 3.8 Model Tuning & Model Training | 19 |
| CHAPTER 4: EXPERIMENTAL ANALYSIS AND RESULTS | 20-30 |
| 4.1 Introduction | 20 |
| 4.2 Environment Setup | 20 |
| 4.3 Parameter Optimization | 20 |
| 4.4 Experimental Result | 20 |
| CHAPTER 5: CONCLUSION AND FUTURE WORK | 31-31 |
| 5.1 Conclusion | 31 |
| 5.2 Future work | 31 |
| REFERENCES | 32-33 |

LIST OF FIGURES

| FIGURES | PAGE NO |
|---|----------------|
| Figure 3.2: Workflow of the proposed model. | 8 |
| Figure 3.6: Transfer learning architecture. | 11 |
| Figure 3.6.1: Convolutional layer | 12 |
| Figure 3.6.2: Pooling Layer | 13 |
| Figure 3.6.3: Fully Connected Layer | 14 |
| Figure 3.7: Pre-trained patient models for patients with lung diseases are shown schematically. | 15 |
| Figure 3.7.1: Architecture of Resnet50 | 16 |
| Figure 3.7.2: Architecture of EfficientNet-B0 | 16 |
| Figure 3.7.3: Architecture of VGG-16 | 17 |
| Figure 3.7.4: Architecture of VGG-19 | 17 |
| Figure 3.7.5: Architecture of Inception-V3 | 18 |
| Figure 3.7.6: Architecture of MobileNet | 18 |
| Figure 4.4.1 ResNet50 Training-Validation Loss and Accuracy | 21 |
| Figure 4.4.2 Confusion Matrix of ResNet50 | 22 |
| Figure 4.4.3 VGG-16 Training-Validation Loss and Accuracy | 23 |

| | |
|---|----|
| Figure 4.4.4 Confusion Matrix of VGG-16 | 23 |
| Figure 4.4.5 EfficientNet Training-Validation Loss and Accuracy | 24 |
| Figure 4.4.6 Confusion Matrix of EfficientNet | 25 |
| Figure 4.4.7 VGG-19 Training-Validation Loss and Accuracy | 26 |
| Figure 4.4.8 Confusion Matrix of VGG-19 | 26 |
| Figure 4.4.9 Inception-V3 Training-Validation Loss and Accuracy | 27 |
| Figure 4.4.10 Confusion Matrix of Inception-V3 | 28 |
| Figure 4.4.11 MobileNet Training-Validation Loss and Accuracy | 29 |
| Figure 4.4.12 Confusion Matrix of MobileNet | 29 |

LIST OF TABLES

| TABLES | PAGE NO |
|--|----------------|
| Table 4.4.1: Test and Train Accuracy of the transfer learning models | 21 |
| Table 4.4.2: Classification Report of ResNet50 | 22 |
| Table 4.4.3: Classification Report of VGG-16 | 24 |
| Table 4.4.4: Classification Report of EfficientNet | 25 |
| Table 4.4.5: Classification Report of VGG-19 | 27 |
| Table 4.4.6: Classification Report of MobileNet | 28 |
| Table 4.4.7: Classification Report of Inception-V3 | 30 |

CHAPTER 1

INTRODUCTION

1.1 Introduction

Common lung diseases such as Lung Cancer, Tuberculosis, Pneumonia and COVID-19 can easily lead to death if early diagnosis and proper treatment are not possible. The first coronavirus was identified in 2019, and it was given the name COVID-19. It was initially discovered in the Chinese city of Wuhan. Then it spread around the world. According to the report dated December 28, 2022, the sickness has impacted 651,918,402 individuals globally, and 6,656,601 have passed away. Fever, coughing, breathing difficulties, etc. are the coronavirus's signs and symptoms. Pneumonia and TB patients are at higher risk. Patients with lung cancer are more at risk than those with TB. Patients with TB and lung cancer may also contract the coronavirus, which can be fatal. Lung cancer is a fatal condition. Uncontrolled cell proliferation in the lung tissues is a feature of lung cancer. It's possible for metastatic disease, surrounding tissue invasion, and an extrapulmonary infection to develop. Most first-stage lung malignancies are lung carcinomas, which develop in the lung's epithelial cells. In terms of cancer-related deaths, lung cancer ranks first among deaths in men and second among deaths in women. Tobacco use is the primary cause of 85% of lung cancers. Those who have never smoked make up the remaining 10-15%.

Tuberculosis is an infectious disease brought on by the Bacterium Mycobacterium Tuberculosis. 1.5 million people died as a result of the illness, which affected one million people globally in 2018. The kingdom is where the term "Tuberculosis" is derived. Patients' rapid weight loss is the main contributor to the deterioration. The lungs are where tuberculosis is most prevalent.

COVID-19, Lung Cancer, Pneumonia, and Tuberculosis can be diagnosed through chest X-ray images. Without Artificial Intelligence, X-ray images may not accurately diagnose any single disease. AI is much faster to detect lung diseases like COVID-19, lung cancer, tuberculosis and pneumonia by using chest X-ray images. If any patient wants to diagnose any disease related to the lung using an X-ray report, the patient will also get a report of other unknown diseases, like, COVID-19, lung cancer, pneumonia, and tuberculosis.

In the future, when we work with other lung-related diseases, it will also be possible to diagnose them easily.

In this study, we collected two labeled datasets of X-ray images of chest to process images of Lung Cancer, Tuberculosis, Pneumonia, COVID-19 and Normal. Deep Transfer learning is used to minimize time on training and optimizing performance of neural networks and used ImageNet's weight in transfer learning. We worked on 5 classes to detect these 4 types of diseases of lung: Lung Cancer, Tuberculosis, Pneumonia and COVID-19. For classifying those diseases, here we used 6 different transfer learning models including, ResNet50, VGG16, EfficientNet, VGG19, MobileNet and InceptionV3.

1.2 Motivation

A chest X-ray report can be used to diagnose lung diseases, but this method should be more accurate and take less time and money. However, it is not specific to any lung-related disease. We were able to work with chest X-ray images of four diseases (Lung Cancer, Tuberculosis, Pneumonia and COVID-19) and finally successfully classify them with high accuracy. These models can be used in a variety of devices and are capable of addressing further issues related to the detection of lung diseases, such as automatically identifying the diseases without the assistance of humans. It'll be less time and money-consuming and more easily, which will be beneficial for the medical sector.

1.3 Research Objective

Nowadays Transfer learning is becoming more popular in many sectors, especially in the medical sector for its image-classifying features more quickly and sufficiently.

In our study, we show how the medical sector can be beneficial using this Deep transfer learning approach. Doctors can quickly and automatically identify diseases of lung like Lung Cancer, Tuberculosis, Pneumonia and COVID-19 from the patient's X-ray report of chest within a very short amount of time with more accuracy which assists them in their treatment in an efficient way. Therefore, we have trained and tested an image dataset of X-ray that contain 5 categories: Normal, Lung Cancer, Tuberculosis, Pneumonia and COVID-19. Transfer learning is used to save time on

training and improve the performance of neural networks. We have got precision, recall, F1-score, and support values of the model from the classification report. We've employed Deep Transfer Learning models including- ResNet50, VGG-16, EfficientNet, VGG-19, MobileNet and InceptionV3. Among them, we have obtained the highest accuracy of 97.65% in ResNet50.

1.4 Rationale of the Study

Most of the studies have dealt with single lung diseases or only COVID-19 and they used images of chest x-ray report. Some studies worked with various lung diseases, but their dataset contained a small amount of data for each disease, which was not enough for a specific diagnosis.

So, we have tried to detect more lung diseases by adding a huge amount of x-ray report of chest images for each disease employing a deep transfer learning approach.

1.5 Organization of the Report

The rest of the report is organized as follows:

Chapter 2 describes the Background of the study, chapter 3 describes the Methodology of the study, chapter 4 describes the Experimental Analysis and Result of the study, chapter 5 describes the Conclusion and Future Work of the study and finally in the References.

CHAPTER 2

BACKGROUND STUDY

2.1 Related Works

Over the generations, a number of researchers have conducted several studies on the recognition of various diseases employing chest x-ray data. Additionally, their efforts have limitations. We shall learn about the researchers' methods, the number of chest x-ray pictures they utilized, the diagnoses they worked on, the models they employed, and their accomplishments in the "background study" section. Their shortcomings and the extent of their improvement are thus made clear.

2.2 Research Summary

Since then, we've studied how chest X-ray pictures may be used to diagnose conditions including pneumonia, lung cancer, Covid-19, and tuberculosis. As a result, we looked at some of the study publications from scientists who had previously researched these disorders using x-ray pictures of chest.

Haritha et al.[1] wanted to identify COVID-19 from images of Chest X-ray with Deep Learning. They employed CheXNet model with chest x-ray pictures. With additional advancements, their concept might be used in real-time COVID-19 detection settings. They used a dataset which contains 1824 chest x-ray images from balanced COVID19 and non-COVID19 classes. They trained their DenseNet121 model on 1824 images and achieved 99.9% accuracy.

Awan et al.[2] wanted to identify COVID-19 from the report of x-ray of chest images using deep learning. They used a dataset of 354 photos of x-ray report of chest. Three models—InceptionV3, VGG19, and ResNet50—were utilized, and accuracy rates of 97%, 98.55%, and 98.55% were obtained.

Brunese et al.[3] wanted to identify COVID-19 and Pulmonary disease using x-ray photos of chest employing explainable deep learning. By utilizing the VGG-16 model, they suggest and assess a transfer learning-based strategy. They created 2 models. First one was designed to determine

whether chest X-rays were taken from healthy people or those with common lung disease. If tagged with common lung disease, input X-rays into a second model to determine if the lung disease is COVID-19. They analyzed a combined total of 6,523 chest X-ray images from two distinct data sets, and their results demonstrated an accuracy of 0.96 for distinguishing between individuals with healthy lungs and those with general pulmonary illness, as well as a 0.98 accuracy to detect COVID-19.

Gouda et al.[4] wanted to identify covid19 using x-ray photos of chest and implemented deep learning techniques. For training and testing, they used a collection of 2790 CXR pictures that contained 930 Covid-19 chest radiography files. It came from a portion of the COV-PEN dataset. Their accuracy was 99.63% using the neural network model ResNet-50. They also promise to do better in the future.

Hasantabar et al. [5] wanted to diagnose and identify contaminated COVID-19 patient tissue using x-ray photos employing CNN techniques. Using lung X-ray images, they used 3 types of deep learning-based models. They presented two techniques, including a DNN for fractal properties of images and CNN approach to diagnose conditions using lung scans directly. They significantly outperformed the DNN technique in terms of accuracy, achieving greater accuracy utilizing CNN architecture (accuracy 93.2% and sensitivity 96.1%). In order to locate sick tissue in lung pictures, they presented a CNN architecture and demonstrated that it can do so with an accuracy of 83.84%.

Phankokkruad [6] wanted to detect coronavirus and pneumonia using x-ray photos of chest. They used 323 COVID-19-positive x-ray photos as dataset. They applied transfer learning methods including, Inception-ResNet-V2, VGG16, and Xception, although CNN models had greater accuracy ratings than the others.

Abraham et al. [7] wanted to detect COVID-19 from x-ray photos using Bayesnet classifier and multi-CNN. Through experiments, they were able to prove that pre-trained multi-CNN outperformed single-CNN at detection of COVID-19. Their technique combines data obtained

from several CNNs with a correlation-based feature selection algorithm and BayesNet classifier to predict COVID-19. They used two public datasets and achieved an highest accuracy of 97.44%.

Ausawalaithong et al.[8] wanted to predict lung cancer using x-ray photos of chest by employing deep learning methods. Both ChestX-ray14 Dataset and JSRT dataset were utilized by them. There were 247 chest photos in the JSRT collection. This dataset contains 154 photos of lung cancer. They used the DenseNet-121 model and got accuracy in JSRT $74.43 \pm 6.01\%$ and in ChestX-ray 14 84.02%.

Amyar et al. [9] wanted to identify Pneumonia and COVID19 applied CT photos. They offer an automated categorization segmentation approach for using chest CT imaging. They used a dataset of 1369 patients with various forms of illness. Their findings indicate the technique's incredibly remarkable outcomes, with a dice coefficient for segmentation exceeding 0.88 and an area below the ROC curve for classification over 97%.

Ibrahim et al.'s[10] goal was to identify lung cancer, COVID-19 and pneumonia using x-rays photos of chest by applying deep learning models including, VGG19-CNN, ResNet152-V2 + Bi-GRU, ResNet152-V2 + GRU and ResNet152-V2. With VGG19+CNN, their accuracy was 98.05%. It has given them more precision.

Mahbub et al.'s[11] goal was to use deep characteristics to identify pulmonary abnormalities using x-rays photos of chest which caused by tuberculosis, pneumonia and Covid-19. They created six different datasets and provided a DNN design. To recognize lung defects in CXRs associated with viral illnesses like TB, pneumonia, and Covid-19, they have established a 9-layered DNN. They utilized 3 different, properly categorized datasets which were widely accessible. The accuracy for unhealthy vs. healthy CXR screening obtained by their recommended DNN was 99.76% on TB, 99.87% on Covid-19 and 99.55% on Pneumonia.

Khan et al.[12] wanted to detect COVID19 using x-rays photos of chest based on deep learning methods. They obtained a dataset from Kaggle and used that to find Covid-19. Three previously trained models were used to categorize COVID-19. These are MobileNetV2, NasNetMobile, and

EfficientNetB1. For Covid19, Pneumonia, lung opacity, and normal, they utilized four groups. In EfficientNetB1, they achieved the greatest accuracy of 96.13%.

Mehta et al.[13] wanted to detect Pneumonia, TB and Covid19 using deep transfer learning models and cGAN. COVID-Severe, COVID-Medium, COVID-Mild, Pneumonia, Tuberculosis and Normal are among the six groups they have utilized. Additionally, 1229 chest X-ray pictures were utilized to detect COVID-19. Additionally, they have suggested using cGAN together with a tailored deep-learning technique to divide chest X-ray pictures into six categories. With the help of ResNet50, Xception, and DenseNet-169, the produced pictures were trained. Their best level of accuracy was 93.67%.

Yildirim et al.[14] wanted to identify Covid19 using x-rays photos of chest based on AI and classifiers. They obtained their datasets from Kaggle. Deep models from MobilenetV2, EfficientNet, and Darknet53 have been used. The NCA approach has resulted in a smaller feature map in terms of size. With a 97.1% accuracy rate, they have the highest accuracy.

2.3 Scope & Challenges

None of the research we have studied has met our objectives or expectations. But by dissecting them, we discovered their flaws and areas for development, which has improved our work. A single disease was the focus of the majority of investigations, and there were relatively few datasets available for studies that classified numerous disorders.

During this study, we used x-ray pictures of chest to categorize four distinct types of lung ailments, and we reached a surprising level of accuracy by employing six widely used Deep Transfer Learning models based on our work. Collecting the dataset was really difficult for us. Finally, all of the difficulties have been resolved.

CHAPTER 3

METHODOLOGY

3.1 Introduction

In this chapter, we are going to manifest the process of our creative method for classifying Lung Diseases. There are some main points like- Data Collection, Data Preprocessing, Data Splitting (Dividing the dataset into Train & Test), Performing One Hot Encoding on the labels after converting it into numerical values, Load pre-trained models, Deep transfer learning and finally, Evaluation in conjunction with the equation, graph, table, and description that are pertinent.

3.2 Workflow

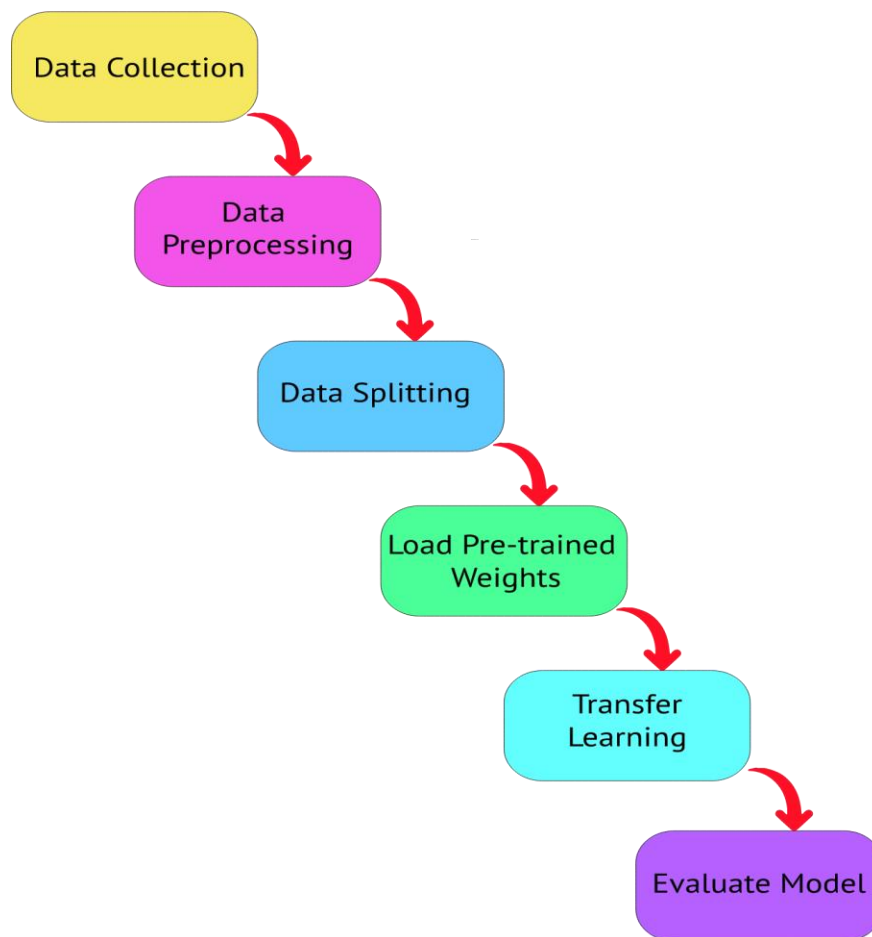


Figure 3.2: Workflow of the proposed model.

Our study has some stages of workflow, including the Data Collection, Preprocessing, Splitting, Load pre-trained models, Transfer Learning and Evaluate models and finally Conclusion and Future Work.

- **Data Collection:** We congregated two different datasets from the internet and processed the raw data to generate our own dataset. There isn't a single dataset accessible because gathering the data was so difficult.
- **Preprocessing of Data:** Then, this data have been analyzed class by class. We faced some noisy and inaccurate data. We manually process such data initially before moving on to the implementation of the selected dataset.
- **Data Splitting:** Following class-by-class processing, data have been shrunk and divided. We had to go through resizing and splitting for training purposes. Data is split across Test (20%) and Train (80%). After converting the labels to numerical values, do one hot encoding on them.
- **Load pre-trained models and apply transfer learning:** By implementing several pre-trained models, we were successful in increasing accuracy. We implement all the models one by one for the training and testing phase. Here, we apply deep CNN-based models called ResNet50, EfficientNet, VGG16, VGG19, InceptionV3, and MobileNet to classify CXR images of lung illnesses.
- **Performance Evaluation:** All data are presented in this part via graphs. We received a few accuracy graphs with validation loss and accuracy after training and testing. Besides, we computed confusion matrix then created a table to display the accuracy. We also showed a measure of f1 and recall in the implementation.
- In the final section, we make a conclusion and describe our future works.

3.3 Data Collection

We congregated two different datasets from the internet and processed the raw data to generate our own dataset. There isn't a single dataset accessible because gathering the data was so difficult. The first dataset was X-Ray of Chest of the patients who are affected by TB, Pneumonia and Covid-19, which contains 7135 images and it has 4 categories including normal, tuberculosis, pneumonia and covid-19. The second dataset was Nodules in Chest X-rays (JSRT) which has the X-ray report of Lung Cancer patients. Following their gathering from those sources, all data have

been analyzed class by class. We faced some noisy and inaccurate data. Before moving on to the implementation of the selected dataset, we manually process such data initially. From the first dataset, we take 4 categories including- NORMAL, PNEUMONIA, COVID-19, TUBERCULOSIS and we take LUNG CANCER from second dataset. After modification, we make our own dataset which has 7,225 images data with these 5 categories.

3.4 Preprocessing of Data

Preprocessing, which is the abstraction of base level in the case of image processing technology, is a typical occurrence with pictures. Primary goal of preprocessing is to reduce unexpected jumble and accentuate a few visual characteristics that are crucial for further processing. Prior to reading the image, we initially conducted our image analysis in order to preprocess our image dataset. Then we reduced the size of our photos, followed by denoising. Our dataset is in its best shape after all phases are successfully completed. The labels of our dataset is 'COVID19', 'NORMAL', 'PNEUMONIA', 'TURBERCULOSIS', 'LUNGCANCER' respectively.

3.5 Data Splitting

To eliminate or significantly minimize bias in training data for machine learning models, dataset splitting is a strategy that is regarded as essential and extremely critical. To avoid overfitting types of machine learning algorithms that can perform badly on real test data, data scientists and analysts constantly go through this procedure. After converting the labels to numerical values, do one hot encoding on them. In this process, we divided our dataset into Train and Test. For the Test, we take 20% and for Train, we take 80% data.

3.6 Deep Transfer Learning Architecture

Machine learning includes deep learning as a sub-branch, which is motivated by brain anatomy. Deep learning techniques are used widely now, and we're seeing really spectacular outcomes in every industry, including image processing in medicine. By utilizing deep learning techniques in the medical field, one obtains important information and patterns from medical data. Many industries, including the data classification, identifying lesions, and data segmentation in the fields of medical sciences, effectively use deep learning techniques. Through the image processing methods of deep learning, it is very easy to classify the image data like- CXR, CT scan, MRI reports etc. Lung cancer, diabetes, skin diseases, brain tumors and other critical disease diagnosis and detection are becoming extremely effective due to this. Deep learning research is spread across several fields. The CNN is responsible for solving the issues associated with image processing which is a subset of the DNN. In CNN function, entering the visual data, computers recognized the image, then it converted into a matrix format that can be handled later. By distinguishing between various visual patterns, the system can categorize the various types of images. The model learns from test pictures when we enter image data for training, and it creates various labels for the input photos. The output may then be estimated using the visual data from the test set, and it is capable of accurately predicting every image in every category. With the use of three separate CNN layers, the CNN primarily analyzes and predicts images. Convolutional layer is the top layer of CNN. The pooling layer is the second layer, followed by the completely connected layer, which is the third layer.

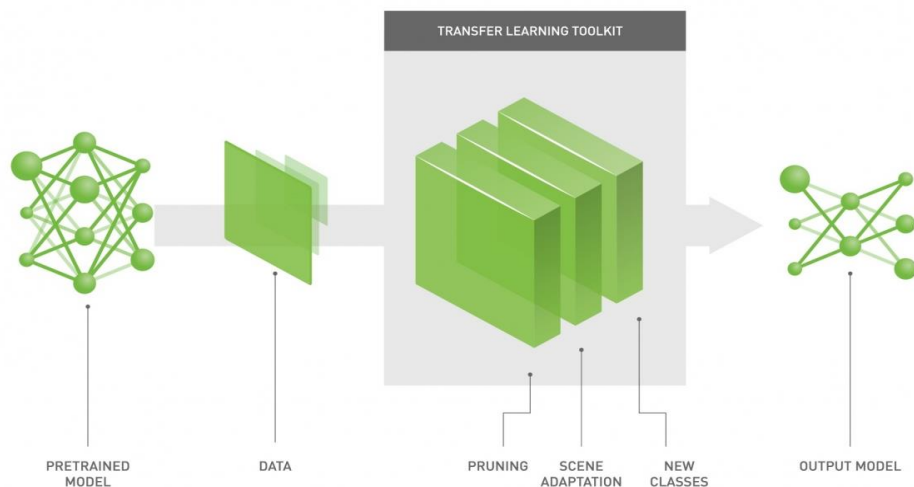


Figure 3.6: Transfer learning architecture.

3.6.1 Convolution Layer

Convolutional Layer is the first layer of the three layers. It forms the foundation for CNN models. It includes visual data patterns. The entered image had been filtered throughout this procedure. A map of functions is made up of values may result from filtering. With the aid of certain kernels, it is possible to apply in this layer and extract both high-level and low-level characteristics from picture data. The Kernel employs a 5*5 and 3*3 transform matrix to determine the input pattern matrix. With the use of the Stride parameter, a filter that compresses the pictures for CNN changes the image's changing motion.

$$x_j^l = f\left(\sum_{a=1}^N w_j^{l-1} * y_a^{l-1} + b_j^l\right)$$

Here, y_a stands in for the layer's a-th feature map, whereas x_j represents the layer's j-th feature map. Here, w_j denotes the j-th kernel, while b_j denotes the bias of the j-th feature map. The vector process for convolution is (*), and N is the total number of features in the layer.

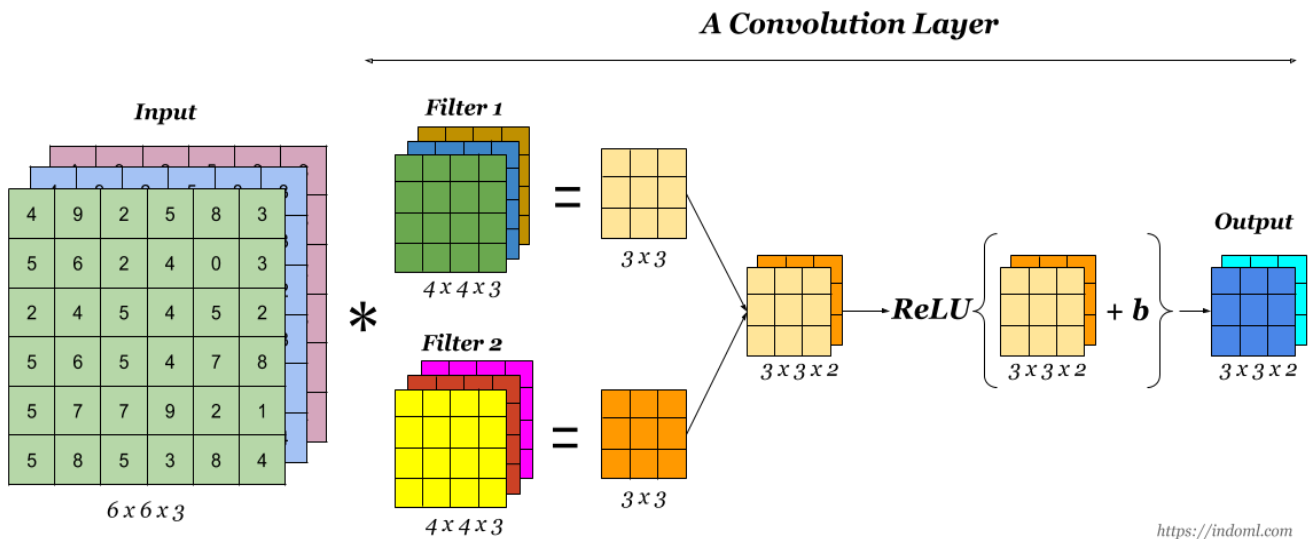


Figure 3.6.1: Convolution layer

3.6.2 Pooling Layer

After that Pooling layer comes next. To decrease number of picture this layer feature maps, increase calculations in mathematics and develop fresh feature maps. CNN has several pooling layers, but we're only utilizing two here. Maximum pooling and a layer of average global pooling. The output neurons are decreased by the maximum pooling layer, which also creates a new feature map of the picture using the maximum values of the image matrix. The fully linked layer is then utilized after the global average pooling layer. It weakens the matrix's data signal. Other layer in between that prevents overfitting as well as network divergence is the dropout layer. It is trained after completing the pooling layer stage.

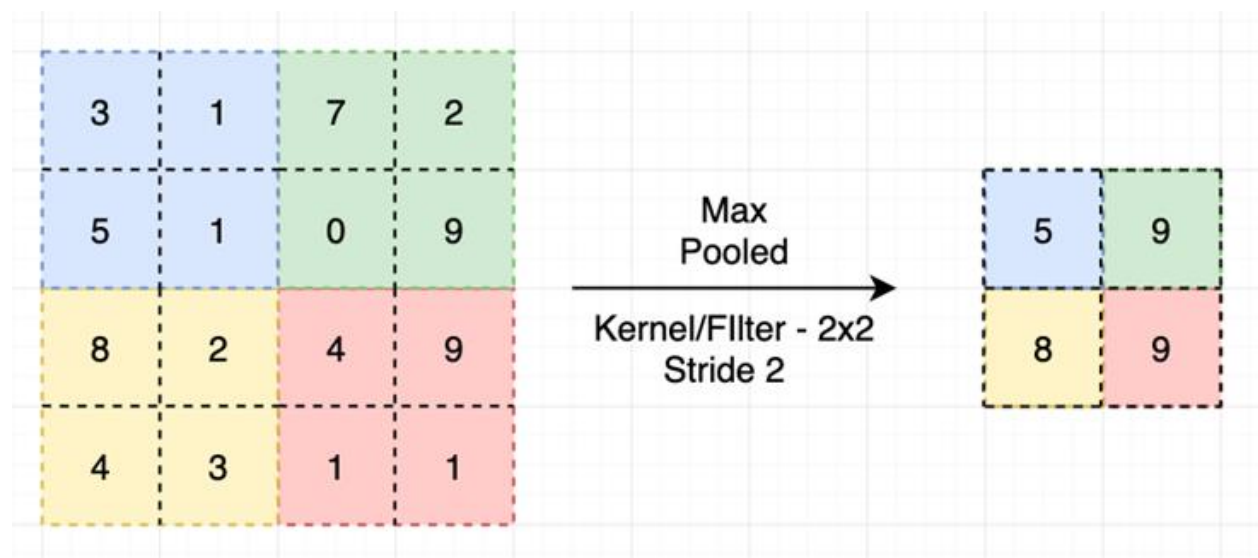


Figure 3.6.2: Pooling Layer

3.6.3 Fully Connected Layer

Final and most important layer on CNN is the fully linked layer. Multilayer backpropagation is being used here. This layer uses two functions, one of which is for output prediction and the other of which is for fully linking all features. Rectified Linear Unit (ReLU) and Softmax are two activation mechanisms that used in a fully connected layer to anticipate the output picture. Equation (i) & (ii) shows the formula of these two activation functions.

$$ReLU(x) = \begin{cases} 0, & x < 0 \\ x, & x \geq 0 \end{cases} \quad \text{----- (i)}$$

$$Soft\ max(x_i) = \frac{e^{x_i}}{\sum_{y=1}^m e^{x_y}} \quad \text{----- (ii)}$$

Here x_i and m , respectively, represent the input data and the number of classes.

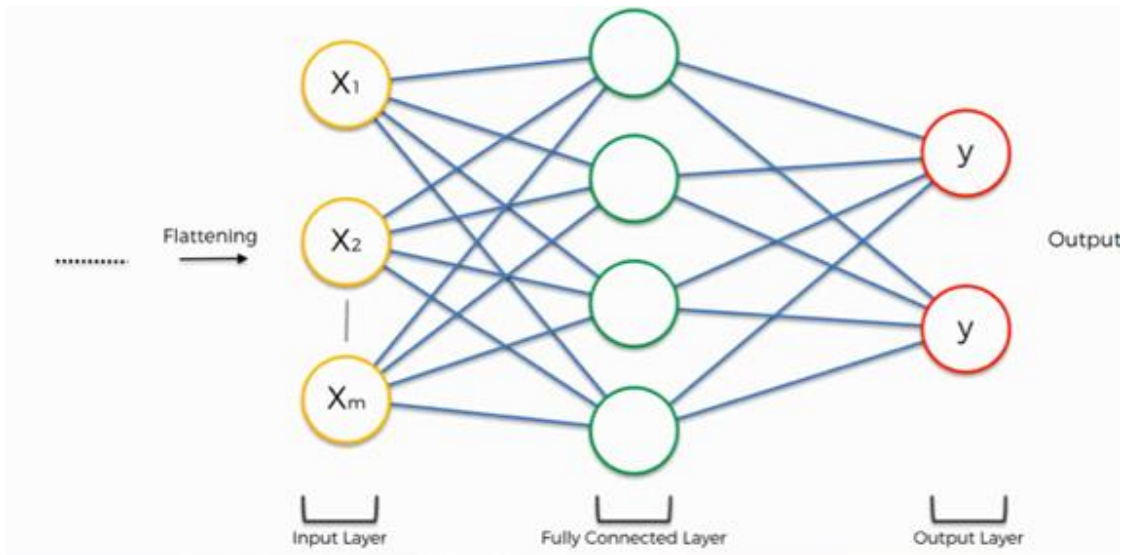


Figure 3.6.3: Fully Connected Layer

3.7 Pre-Trained Models

We are working with datasets for lung disease in this project. Deep learning uses the AI learning processes, hence it occasionally requires a lot of data. However, there is another issue, which is that classifying this dataset by any specialists will take a lot of time and money. On the other hand, while discussing the transfer learning technique, we can observe that this sort of approach requires a more constrained cost for calculations and it allows for fewer datasets to be used for data training. The pre-trained models used a huge dataset to perform the transfer learning process, passing the knowledge to the algorithm to be taught.

Here, we constructed deep CNN-based ResNet50, EfficientNet, VGG16, VGG19, InceptionV3 and MobileNet models to categorize CXR pictures of lung diseases. The paucity of data and training time can be overcome by applying ImageNet data, and we have applied a transfer learning technique for this justification. To forecast common lung diseases, we employed conventional CNN, including pre-trained ResNet50, EfficientNet, VGG16, VGG19, InceptionV3 and MobileNet. Figure 3.7 illustrates everything in this case quite clearly.

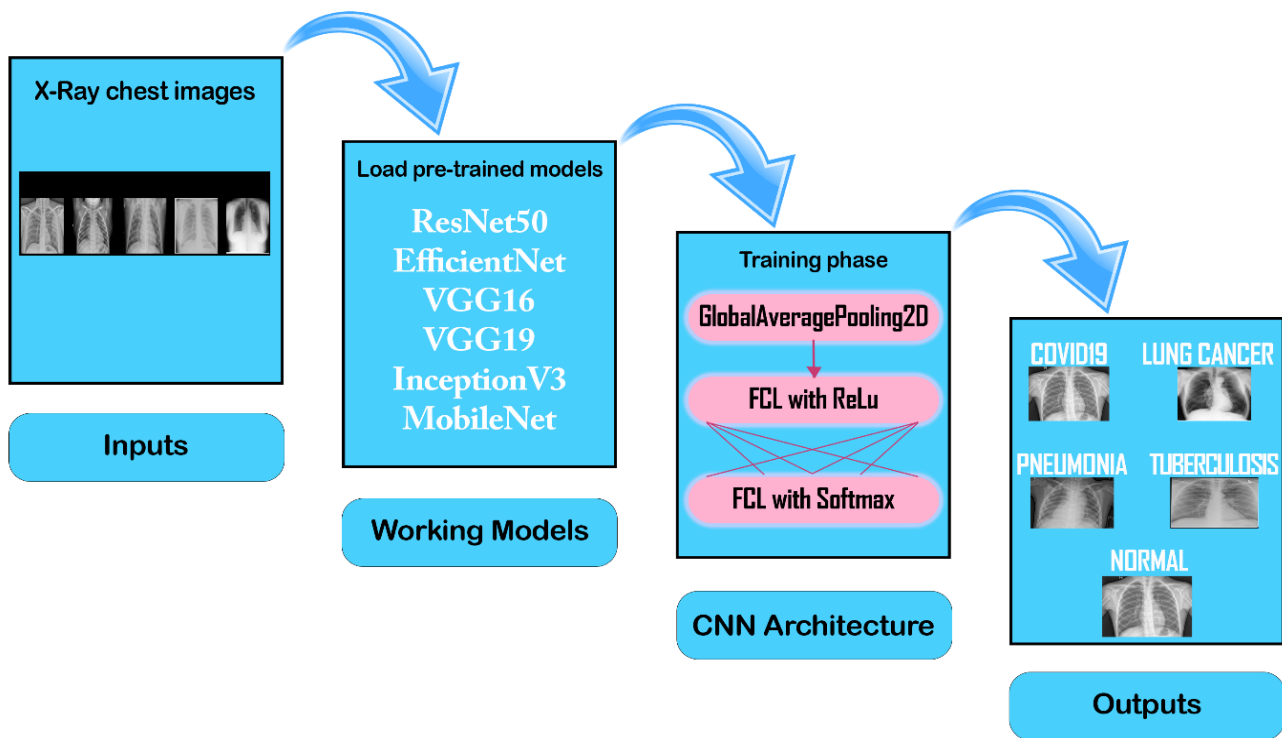
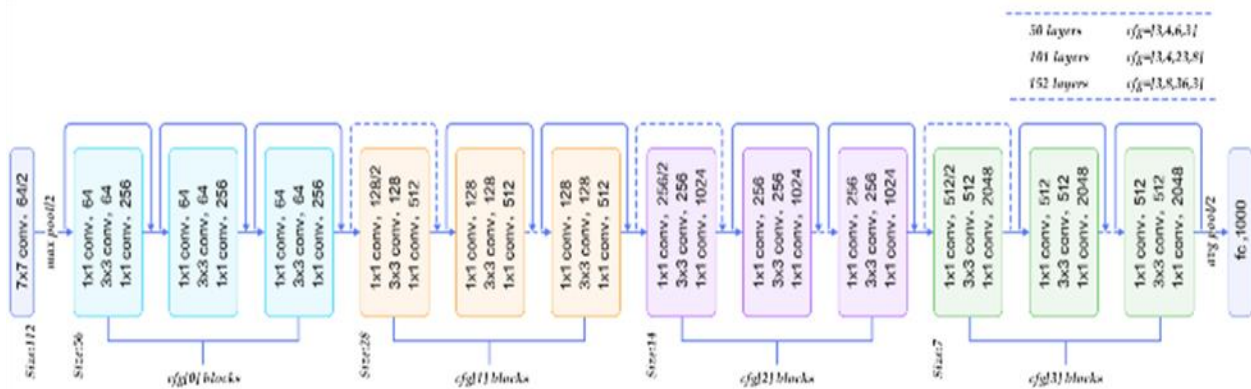


Figure 3.7: Pre-trained patient models for patients with lung diseases are shown schematically.

3.7.1 ResNet50

ResNet or Residual Neural Network is a super powerful convolutional neural network. ResNets are super powerful and it actually won the ‘ImageNet Challenge’ back in 2015. It is a more developed version of the CNN. This prevents the distortion that occurs as the network grows larger and more complex. ResNet50 is a classic neural network used as a backbone for many computer vision tasks. It can be loaded as a pre-trained version of the network trained on more than a million images from the ImageNet database. The pre-trained network can classify images into 1000 object categories. The network has an image input size of 224-by-224 and it has 50 layers.



3.7.2 EfficientNet-B0

Efficientnet-B0 model is one of the EfficientNet models designed to perform image classification. This model was pre-trained in TensorFlow. All the EfficientNet models have been pre-trained on the ImageNet image database. The network has an image input size of 224-by-224.

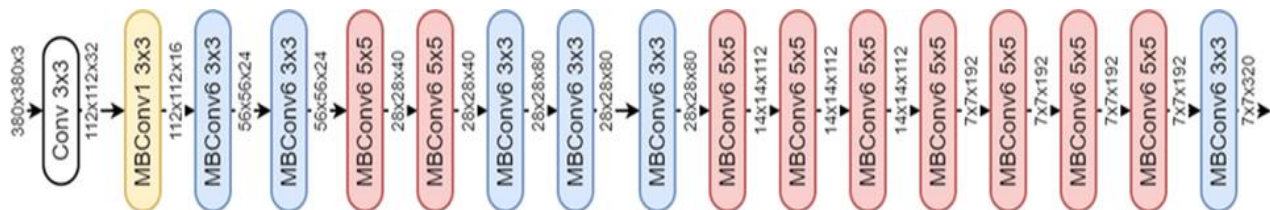


Figure 3.7.2: Architecture of EfficientNet-B0

3.7.3 VGG-16

VGG16 was identified to be the best-performing model on the ImageNet dataset. In the race to enable computers to "view" the world, VGG16 has proven to be a significant turning point. It represents one of the important breakthroughs that opened the door for other achievements in this field to come.

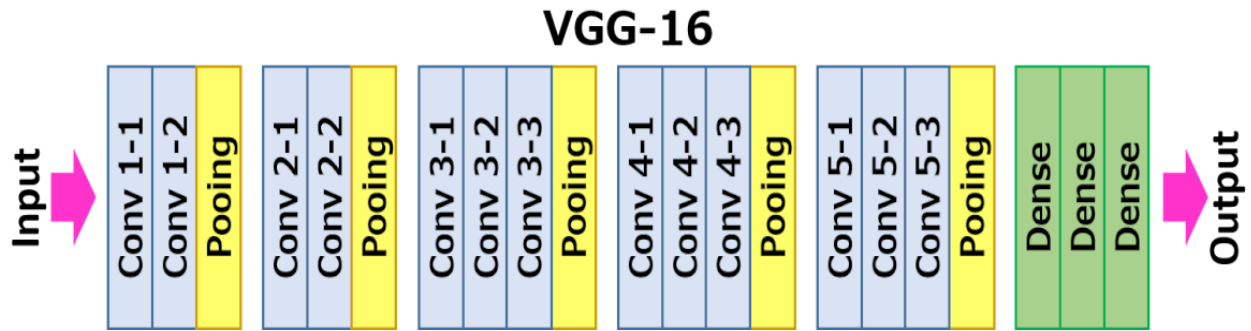


Figure 3.7.3: Architecture of VGG-16

3.7.4 VGG-19

VGG19 is one kind of the model of VGG that has 19 layers where number of convolution layers is 16, and 3 Fully connected layers, 5 MaxPool layers and 1 SoftMax layer. This network got a fixed-size (224 * 224) RGB image as input, suggesting that the matrix was structured (224,224,3).

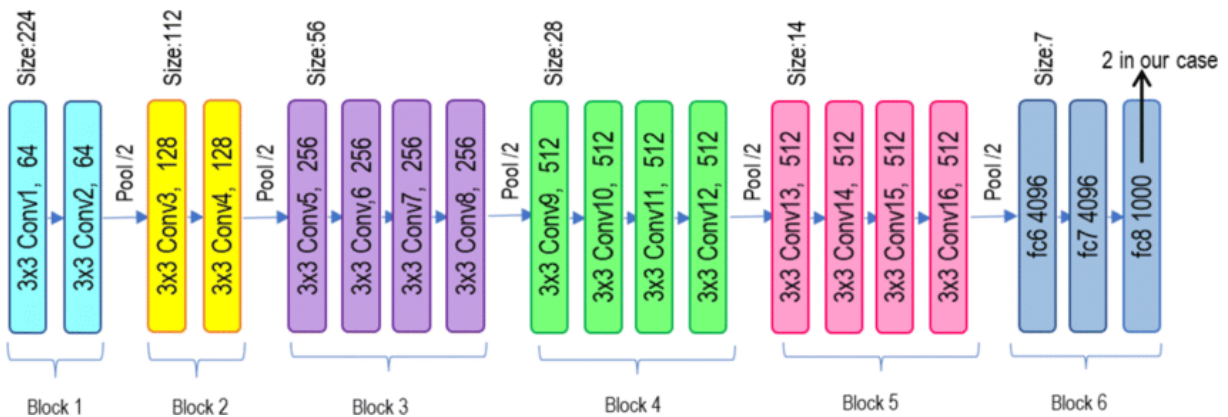


Figure 3.7.4: Architecture of VGG-19

3.7.5 Inception-V3

The updated version, Inception-V3, is comparable to the first Inception-V1. It was known as GoogLeNet in 2014 and it was developed by a team at Google. The Inception-V3 model was released in the year 2015. Its error rate is lower than its forerunners and it has a total of 42 layers.

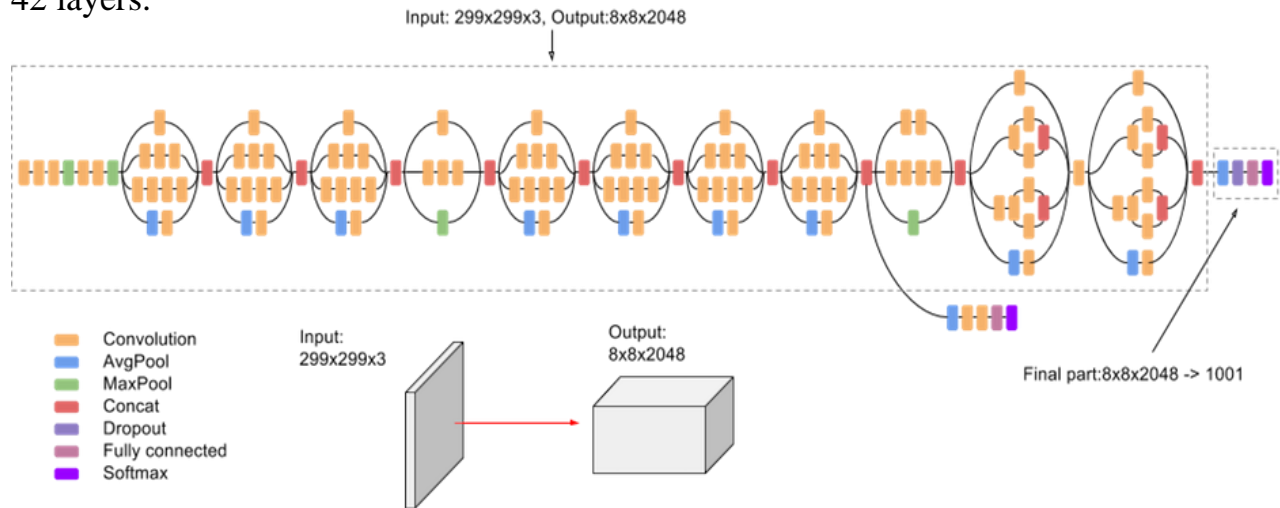


Figure 3.7.5: Architecture of Inception-V3

3.7.6 MobileNet

The MobileNet model has 27 convolutional layers, featuring 13 layers that are depth-dependent, an average pooling layer, a fully connected layer, and a softmax layer. To minimize model size and processing, it substitutes depth-wise separable convolutions for conventional convolutions. As a result, it may be utilized to create compact deep neural networks for embedded and mobile vision applications.

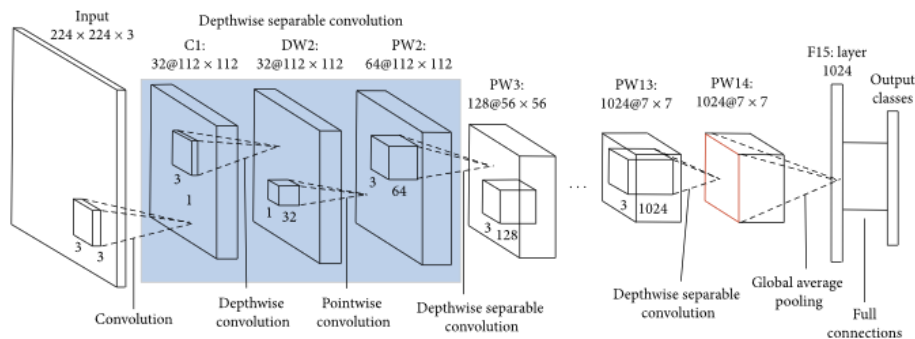


Figure 3.7.6: Architecture of MobileNet

3.8 Model Tuning and Model Training

In essence, tuning involves changing a few hyperparameters through a process of trial and error. We raised batch size to 32 in order to improve the upgraded CNN model. When we extend the epoch to 30, our model significantly improves.

The most crucial component of implementation is model training. Keras and Tensorflow framework have used to implement the CNN model. Here we take 10% data as validation data from the training dataset. Within the training loop, training and validation datasets are loaded. The model is trained utilizing the Adam Optimizer with Cross-Entropy Loss. The model is evaluated on every epoch on the validation set, and the model with the highest validation accuracy is stored for storage for a later evaluation and use. The training and validation error and loss, as well as the plot of error and loss overload, are saved once the training is finished. Here we use Callbacks that are essential when we want to control the training of a model. Callbacks help us prevent overfitting, visualize our training progress, save checkpoints and much more.

CHAPTER 4

EXPERIMENTAL ANALYSIS AND RESULTS

4.1 Introduction

At this point, we'll talk over the confusion matrix and model accuracy analysis. For each, a plot diagram is also included. Several CNN models, including ResNet50, EfficientNet, VGG16, VGG19, InceptionV3, and MobileNet, were employed to categorize the results. We used those models and ran separate tests on our dataset to determine which had the best accuracy.

4.2 Environment Setup

Our implementation is carried out on a PC running Windows 11 with a 12th Gen Intel(R) Core(TM) i7-12700 2.10 GHz CPU, NVIDIA GeForce RTX 2060 graphics card, and 16 GB of RAM. The model is run using Google Colab Notebook, an open-source platform. The model is put into practice using the Keras and Tensorflow frameworks.

4.3 Parameter Optimization

We focused on a few factors throughout the simulation of our suggested model so that it can improve its efficiency. The batch size has been raised from 16 to 32. It improved the performance of our model. It didn't significantly increase our results even after attempting up to 15 epochs. Thus, 30 epochs were used. We employed "ReLU" and "Softmax" as classification algorithms, both of which are activation functions, in the case of the activation function. minimizing training loss.

4.4 Experimental Results

We applied the transfer learning strategy and constructed our own neural network. We proposed six different architectures for transfer learning. including- ResNet50, EfficientNet, VGG-16, VGG-19, InceptionV3, and MobileNet.

The following Table-4.4.1 compares the final training accuracy comparison of several models.

TABLE 4.4.1: TEST AND TRAIN ACCURACY OF THE TRANSFER LEARNING MODELS

| Pre-trained Models | Test Accuracy | Train Accuracy |
|--------------------|---------------|----------------|
| ResNet50 | 0.9765 | 0.9967 |
| VGG16 | 0.9744 | 0.9938 |
| EfficientNet | 0.9723 | 0.9941 |
| VGG19 | 0.9682 | 0.9926 |
| MobileNet | 0.9433 | 0.9891 |
| Inception-V3 | 0.9073 | 0.9306 |

Here, ResNet50 outperformed among those models and it achieved an accuracy of 0.9765.

Here in Figure 4.4.1 graph is used to show Training-Validation Loss and Training-Validation Accuracy of the ResNet50. In the first section, it represents Train Loss & Validation Loss. In the second section, it represents Training Accuracy & Validation Accuracy. The orange line represents Validation Loss and Accuracy, whereas the blue line represents Training Loss and Training Accuracy.

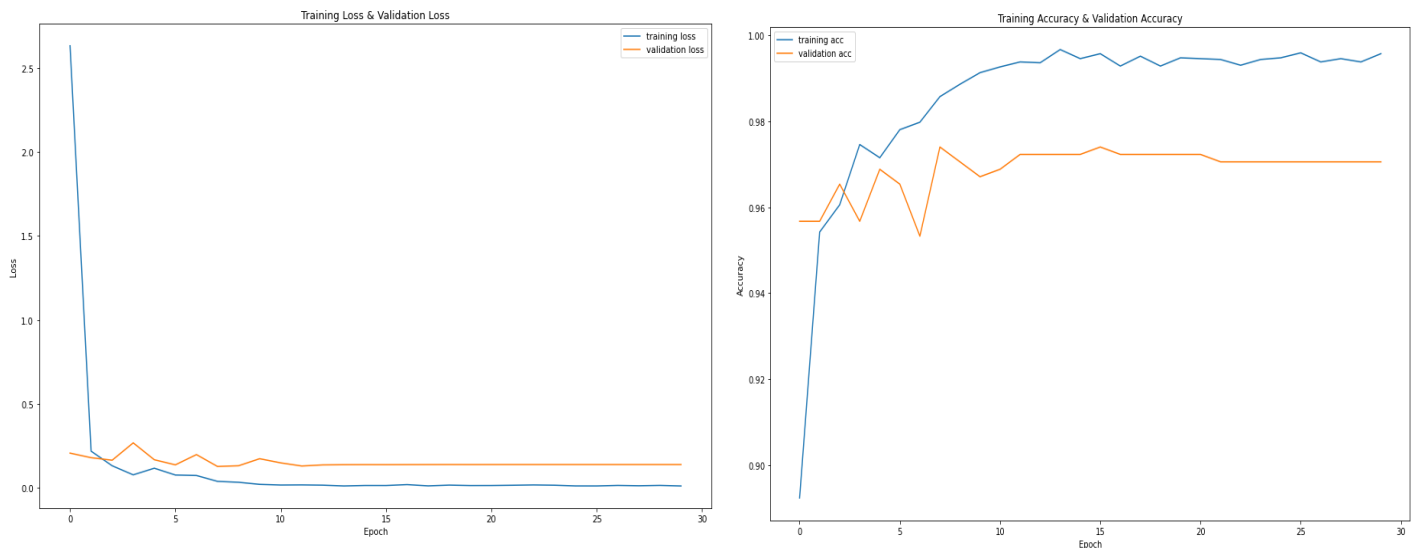


Figure 4.4.1 ResNet50 Training-Validation Loss and Accuracy.

Error occurs when an algorithm encounters data conflict. Though this model is selected as the best model of our study still it has certain mistakes because of the limitation of the technology. Machine gets confused when the term is to identify disease or categorize many types of classes. Here a total of 34 data conflicts are shown in fig 4.4.2. Covid19 class has 0 conflicts with Normal, 2 with Pneumonia, 1 with Tuberculosis and 1 with Lung Cancer class. Normal class has 0 conflict with Covid19, 17 with Pneumonia and 0 with both Tuberculosis and Lung Cancer. Pneumonia class has 2 conflicts with Covid19, 11 with Normal and 0 with both Tuberculosis and Lung Cancer. Tuberculosis class and Lung Cancer class does not have any data conflicts with rest of the classes.

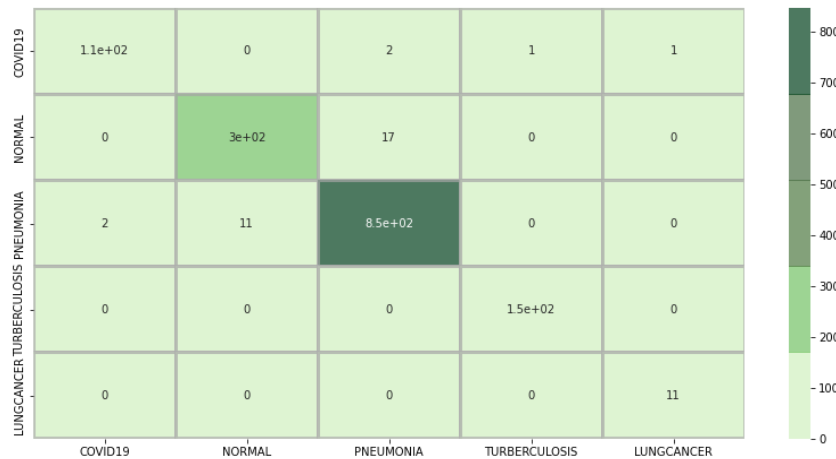


Figure 4.4.2 Confusion Matrix of ResNet50

For the ResNet50 model, the Precision, Recall and F1-score are shown below. Here 0 to 4 are indicates ‘COVID19’, ‘NORMAL’, ‘PNEUMONIA’, ‘TUBERCULOSIS’, ‘LUNG CANCER’ labels respectively.

TABLE 4.4.2: CLASSIFICATION REPORT OF RESNET50

| | Precision | Recall | F1-score | Support |
|---------------------|-----------|--------|----------|---------|
| 0 | 0.98 | 0.96 | 0.97 | 114 |
| 1 | 0.96 | 0.95 | 0.96 | 315 |
| 2 | 0.98 | 0.98 | 0.98 | 859 |
| 3 | 0.99 | 1.00 | 1.00 | 146 |
| 4 | 0.92 | 1.00 | 0.96 | 11 |
| Accuracy | | | 0.98 | 1445 |
| Macro avg | 0.97 | 0.98 | 0.97 | 1445 |
| Weighted avg | 0.98 | 0.98 | 0.98 | 1445 |

Here, Figure 4.4.3 graph is used to show Training-Validation Loss and Training-Validation Accuracy of the VGG16. In the first section, it represents Train Loss & Validation Loss. In the second section, it represents Training Accuracy & Validation Accuracy. The orange line represents Validation Loss and Accuracy, whereas the blue line represents Training Loss and Training Accuracy.

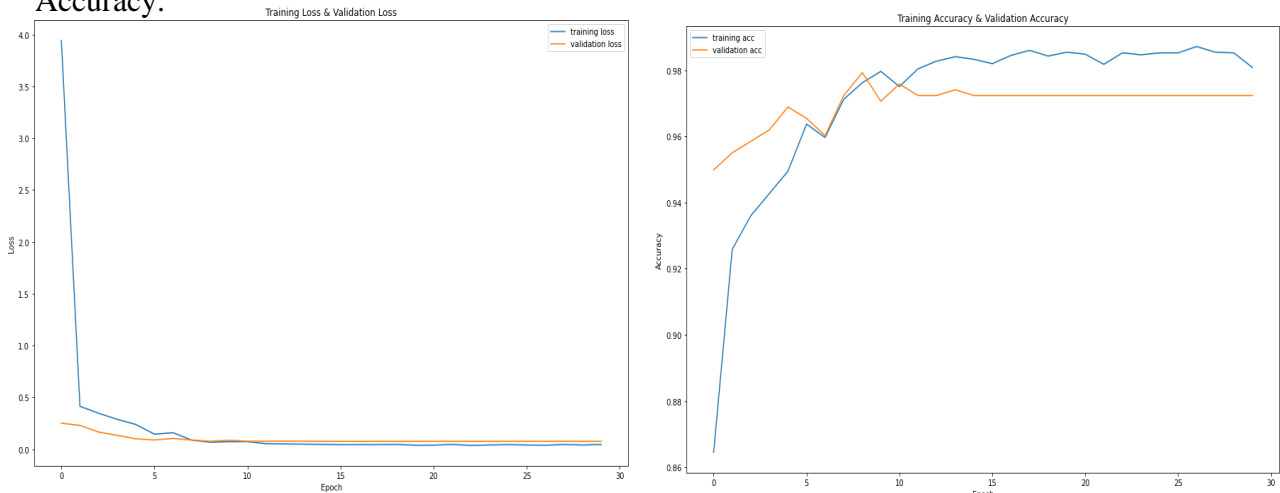


Fig. 4.4.3 VGG-16 Training-Validation Loss and Accuracy.

Here a total of 37 data conflicts are shown in fig 4.4.4. Covid19 class has 0 conflicts with Normal, 3 conflicts with Pneumonia, 2 with Tuberculosis and 0 with Lung Cancer class. Normal class has 0 conflict with Covid19, 17 with Pneumonia and 0 conflicts with both Tuberculosis and Lung Cancer. Pneumonia class has 15 conflicts with Normal, 0 with Covid19, Tuberculosis and Lung Cancer class. Tuberculosis class and Lung Cancer class does not have any data conflicts with rest of the classes.

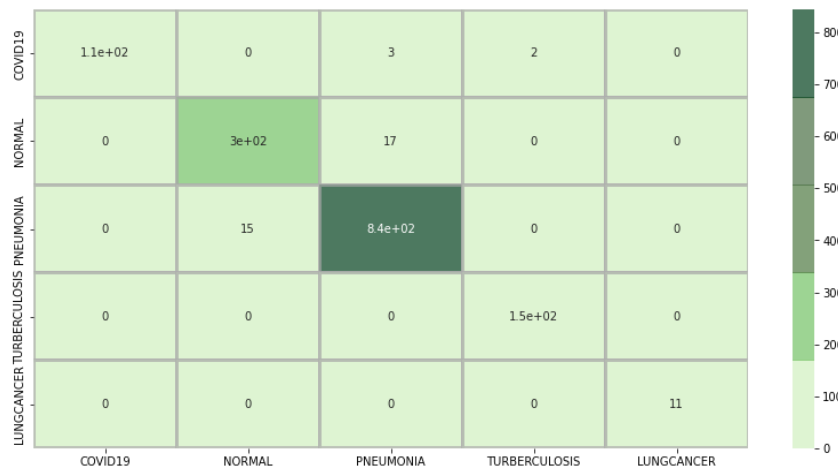


Fig. 4.4.4 Confusion Matrix of VGG-16

For the VGG16 model, the Precision, Recall and F1-score are shown below. Here 0 to 4 are indicates ‘COVID19’, ‘NORMAL’, ‘PNEUMONIA’, ‘TUBERCULOSIS’, ‘LUNG CANCER’ labels respectively.

TABLE 4.4.3: CLASSIFICATION REPORT OF VGG16

| | Precision | Recall | F1-score | Support |
|---------------------|-----------|--------|----------|---------|
| 0 | 1.00 | 0.96 | 0.98 | 114 |
| 1 | 0.95 | 0.95 | 0.95 | 315 |
| 2 | 0.98 | 0.98 | 0.98 | 859 |
| 3 | 0.99 | 1.00 | 0.99 | 146 |
| 4 | 1.00 | 1.00 | 1.00 | 11 |
| Accuracy | | | 0.97 | 1445 |
| Macro avg | 0.98 | 0.98 | 0.98 | 1445 |
| Weighted avg | 0.97 | 0.97 | 0.97 | 1445 |

Here, Figure 4.4.5 graph is used to show Training-Validation Loss and Training-Validation Accuracy of the EfficientNet. In the first section, it represents Train Loss & Validation Loss. In the second section, it represents Training Accuracy & Validation Accuracy. The orange line represents Validation Loss and Accuracy, whereas the blue line represents Training Loss and Training Accuracy.

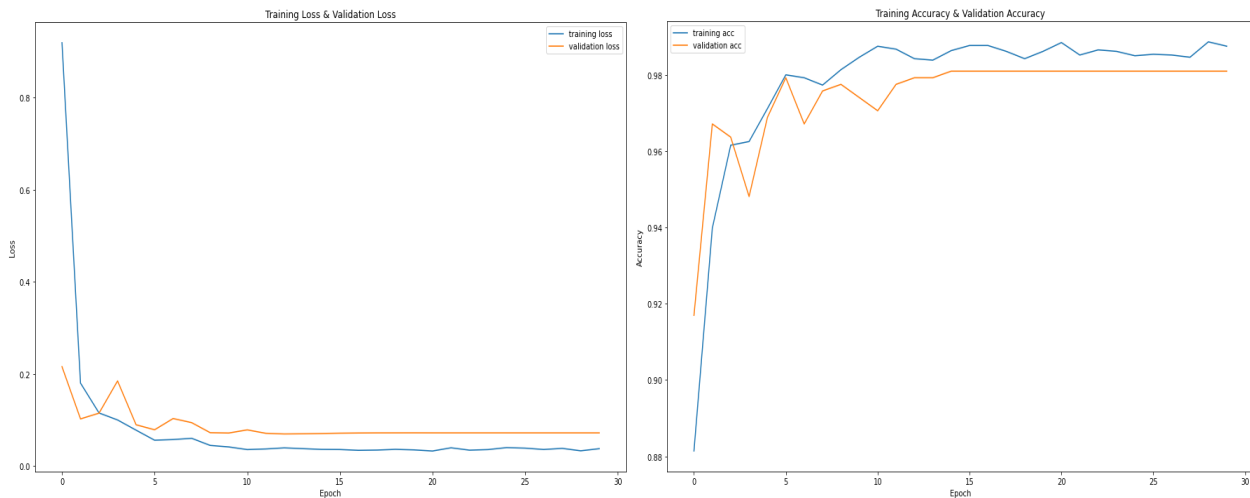


Fig. 4.4.5 EfficientNet Training-Validation Loss and Accuracy.

Here a total of 50 data conflicts are shown in fig 4.4.6. Covid19 class has 0 conflicts with Normal, 1 conflict with Pneumonia, 2 with Tuberculosis and 0 with Lung Cancer class. Normal class has 0 conflict with Covid19, 17 with Pneumonia and 0 conflicts with both Tuberculosis and Lung Cancer. Pneumonia class has 19 conflicts with Normal, 0 with Covid19, Tuberculosis and Lung Cancer class. Tuberculosis class has 1 conflict with Lung Cancer and 0 conflict with rest of all classes. Lung Cancer class does not have any data conflicts with rest of the classes.

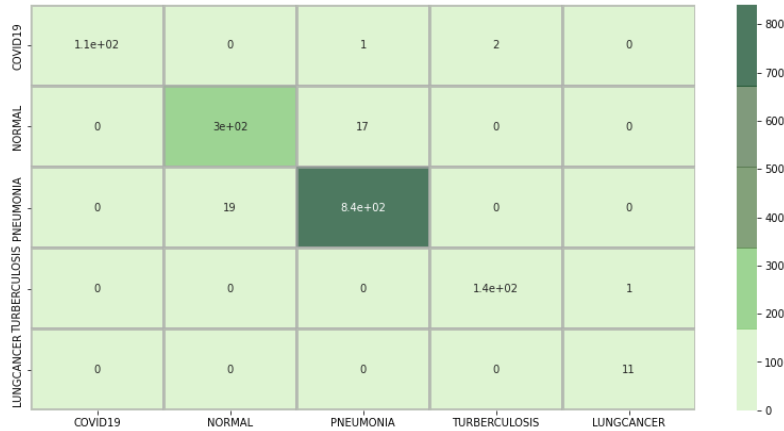


Fig. 4.4.6 Confusion Matrix of EfficientNet

For the EfficientNet model, the Precision, Recall and F1-score are shown below. Here 0 to 4 are indicates ‘COVID19’, ‘NORMAL’, ‘PNEUMONIA’, ‘TUBERCULOSIS’, ‘LUNG CANCER’ labels respectively.

TABLE 4.4.4: CLASSIFICATION REPORT OF EFFICIENTNET

| | Precision | Recall | F1-score | Support |
|---------------------|-----------|--------|----------|---------|
| 0 | 1.00 | 0.97 | 0.99 | 114 |
| 1 | 0.94 | 0.95 | 0.94 | 315 |
| 2 | 0.98 | 0.98 | 0.98 | 859 |
| 3 | 0.99 | 0.99 | 0.99 | 146 |
| 4 | 0.92 | 1.00 | 0.96 | 11 |
| Accuracy | | | 0.97 | 1445 |
| Macro avg | 0.96 | 0.98 | 0.97 | 1445 |
| Weighted avg | 0.97 | 0.97 | 0.97 | 1445 |

Here, Figure 4.4.7 graph is used to show Training-Validation Loss and Training-Validation Accuracy of the EfficientNet. In the first section, it represents Train Loss & Validation Loss. In the second section, it represents Training Accuracy & Validation Accuracy. The orange line represents Validation Loss and Accuracy, whereas the blue line represents Training Loss and Training Accuracy.

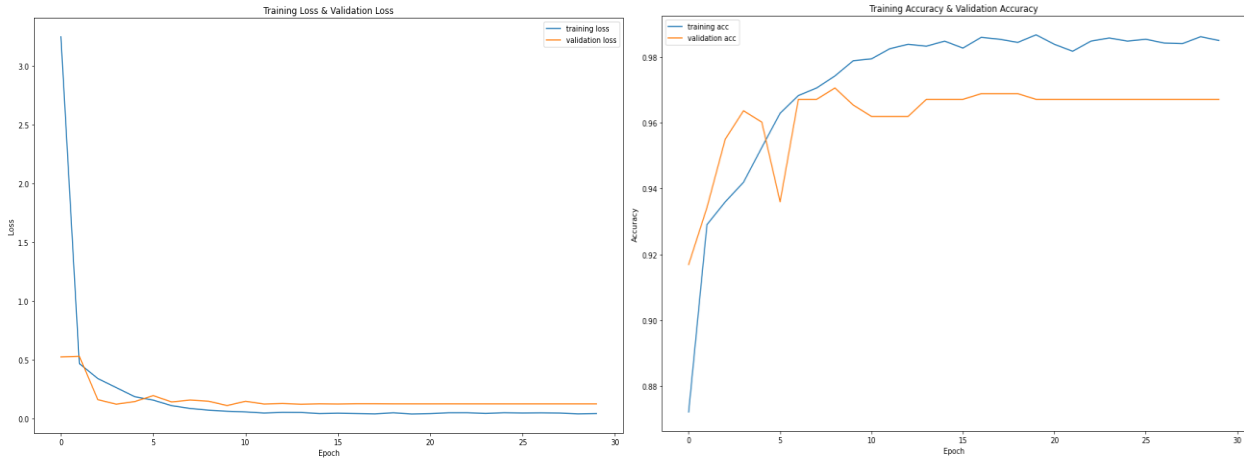


Fig. 4.4.7 VGG-19 Training-Validation Loss and Accuracy.

Here a total of 46 data conflicts are shown in fig 4.4.8. Covid19 class has 0 conflicts with Normal, 3 conflict with Pneumonia, 4 with Tuberculosis and 0 with Lung Cancer class. Normal class has 1 conflict with Covid19, 26 with Pneumonia and 0 conflicts with both Tuberculosis and Lung Cancer. Pneumonia class has 10 conflicts with Normal, 0 with Covid19, Tuberculosis and Lung Cancer class. Tuberculosis class has 2 conflicts with Covid19 and 0 conflict with rest of all classes. Lung Cancer class does not have any data conflicts with rest of the classes.

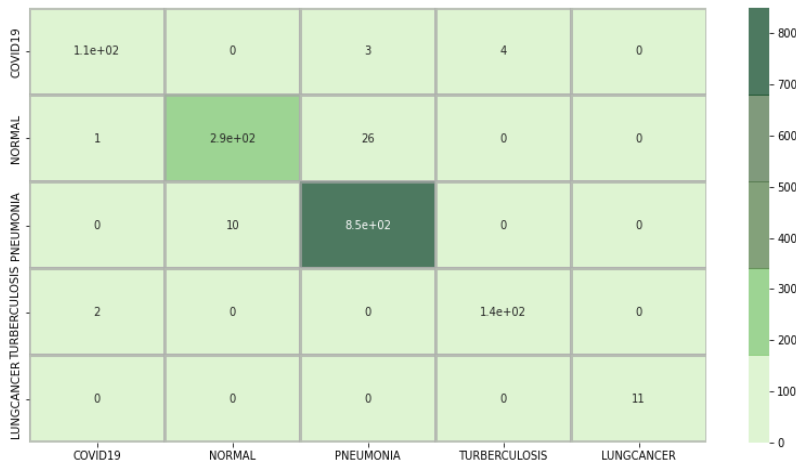


Fig. 4.4.8 Confusion Matrix of VGG-19

For the VGG19 model, the Precision, Recall and F1-score are shown below. Here 0 to 4 are indicates ‘COVID19’, ‘NORMAL’, ‘PNEUMONIA’, ‘TUBERCULOSIS’, ‘LUNG CANCER’ labels respectively.

TABLE 4.4.5: CLASSIFICATION REPORT OF VGG19

| | Precision | Recall | F1-score | Support |
|---------------------|-----------|--------|----------|---------|
| 0 | 0.97 | 0.94 | 0.96 | 114 |
| 1 | 0.97 | 0.91 | 0.94 | 315 |
| 2 | 0.97 | 0.99 | 0.98 | 859 |
| 3 | 0.97 | 0.99 | 0.98 | 146 |
| 4 | 1.00 | 1.00 | 1.00 | 11 |
| Accuracy | | | 0.97 | 1445 |
| Macro avg | 0.98 | 0.97 | 0.97 | 1445 |
| Weighted avg | 0.97 | 0.97 | 0.97 | 1445 |

Here, Figure 4.4.9 graph is used to show Training-Validation Loss and Training-Validation Accuracy of the MobileNet. In the first section, it represents Train Loss & Validation Loss. In the second section, it represents Training Accuracy & Validation Accuracy. The orange line represents Validation Loss and Accuracy, whereas the blue line represents Training Loss and Training Accuracy.

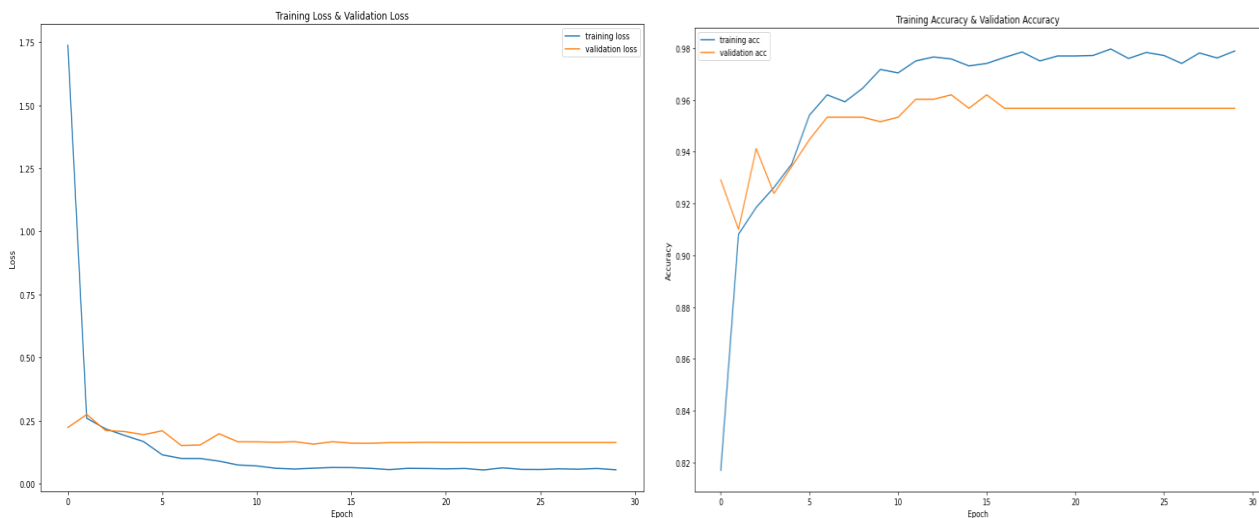


Fig. 4.4.9 MobileNet Training-Validation Loss and Accuracy.

Here a total of 82 data conflicts are shown in fig 4.4.10. Covid19 class has 0 conflicts with Normal, 11 conflict with Pneumonia, 7 with Tuberculosis and 0 with Lung Cancer class. Normal class has 2 conflicts with Covid19, 36 with Pneumonia and 0 conflicts with both Tuberculosis and Lung Cancer. Pneumonia class has 1 conflict with Covid19, 24 with Normal, 0 with both Tuberculosis and Lung Cancer class. Tuberculosis class has 1 conflict with Pneumonia and 0 conflict with rest of all classes. Lung Cancer class does not have any data conflicts with rest of the classes.

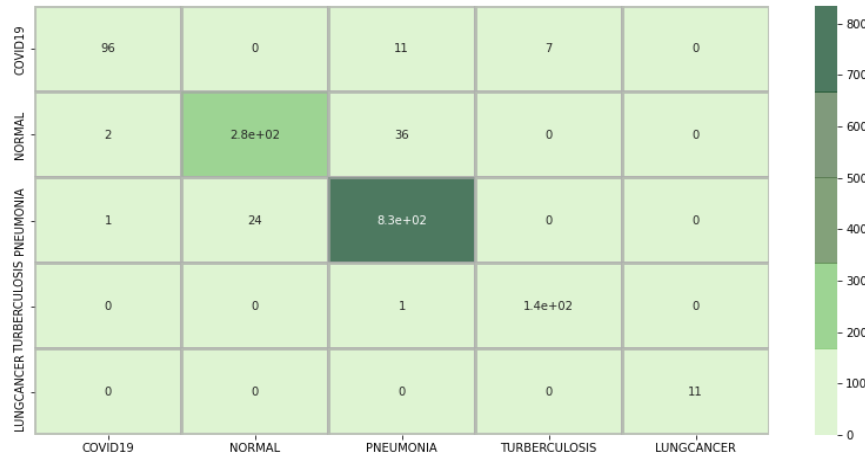


Fig. 4.4.10 Confusion Matrix of MobileNet

For the MobileNet model, the Precision, Recall and F1-score are shown below. Here 0 to 4 are indicates ‘COVID19’, ‘NORMAL’, ‘PNEUMONIA’, ‘TUBERCULOSIS’, ‘LUNG CANCER’ labels respectively.

TABLE 4.4.6: CLASSIFICATION REPORT OF MOBILENET

| | Precision | Recall | F1-score | Support |
|---------------------|-----------|--------|----------|---------|
| 0 | 0.97 | 0.84 | 0.90 | 114 |
| 1 | 0.92 | 0.88 | 0.90 | 315 |
| 2 | 0.95 | 0.97 | 0.96 | 859 |
| 3 | 0.95 | 0.99 | 0.97 | 146 |
| 4 | 1.00 | 1.00 | 1.00 | 11 |
| Accuracy | | | 0.94 | 1445 |
| Macro avg | 0.96 | 0.94 | 0.95 | 1445 |
| Weighted avg | 0.94 | 0.94 | 0.94 | 1445 |

Here, Figure 4.4.11 graph is used to show Training-Validation Loss and Training-Validation Accuracy of the Inception-V3. In the first section, it represents Train Loss & Validation Loss. In the second section, it represents Training Accuracy & Validation Accuracy. The orange line represents Validation Loss and Accuracy, whereas the blue line represents Training Loss and Training Accuracy.

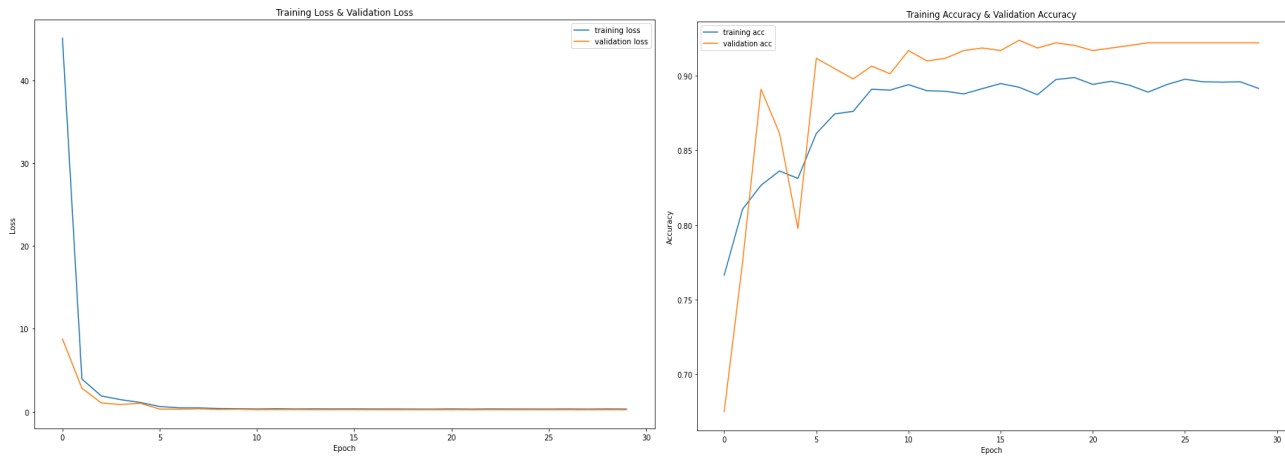


Fig. 4.4.11 Inception-V3 Training-Validation Loss and Accuracy.

Here a total of 134 data conflicts are shown in fig 4.4.12. Covid19 class has 1 conflict with Normal, 13 conflicts with Pneumonia, 12 with Tuberculosis and 1 with Lung Cancer class. Normal class has 5 conflicts with Covid19, 34 with Pneumonia and 1 conflict with Tuberculosis and 0 conflict with Lung Cancer. Pneumonia class has 5 conflicts with Covid19, 38 with Normal, 2 with Tuberculosis and 0 with Lung Cancer class. Tuberculosis class has 8 conflicts with Covid19, 2 with Normal, 9 with Pneumonia and 1 with Lung Cancer class. Lung Cancer class has 1 conflict with Covid19, 1 with Tuberculosis, 0 with both Normal and Pneumonia.

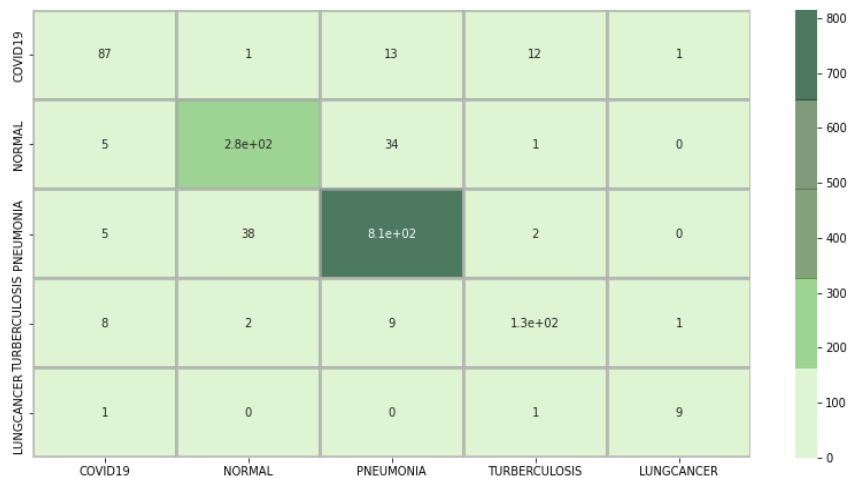


Fig. 4.4.12 Confusion Matrix of Inception-V3

For the Inception-V3 model, the Precision, Recall and F1-score are shown below. Here 0 to 4 are indicates ‘COVID19’, ‘NORMAL’, ‘PNEUMONIA’, ‘TUBERCULOSIS’, ‘LUNG CANCER’ labels respectively.

TABLE 4.4.7: CLASSIFICATION REPORT OF INCEPTION-V3

| | Precision | Recall | F1-score | Support |
|---------------------|------------------|---------------|-----------------|----------------|
| 0 | 0.82 | 0.76 | 0.79 | 114 |
| 1 | 0.87 | 0.87 | 0.87 | 315 |
| 2 | 0.94 | 0.95 | 0.94 | 859 |
| 3 | 0.89 | 0.86 | 0.88 | 146 |
| 4 | 0.82 | 0.82 | 0.82 | 11 |
| Accuracy | | | 0.91 | 1445 |
| Macro avg | 0.87 | 0.85 | 0.86 | 1445 |
| Weighted avg | 0.91 | 0.91 | 0.91 | 1445 |

CHAPTER 5

CONCLUSION AND FUTURE WORK

5.1 Conclusion

The major focus of this work was the identification of 4 common types of lung diseases including-COVID-19, Pneumonia, Tuberculosis and Lung Cancer. In this study, It is suggested that utilizing images of the chest X-ray, Deep Transfer Learning methods be used to automatically identify COVID-19, Pneumonia, Lung Cancer, and Tuberculosis. Many different Deep Learning Algorithms exist for various picture categorization issues. The ResNet50 model produced the best accuracy out of all the Deep Transfer Learning models we implemented. And to identify four lung diseases, we trained and tested a huge number of chest X-rays images. By validating multiple models, we found the highest accuracy rate for four lung disease detection when compared to our previous studies.

5.2 Future work

In the future our target is to extend our implementation with more huge datasets related to lung diseases. We will work with more lung diseases along with these 4 types of diseases. Further, the computational time may be reduced by using various portable Deep-Learning methods. Additionally, to increase efficiency, it is possible to choose the best features for classification by using optimization techniques, particularly metaheuristic approaches. This will be very beneficial for the medical sector in making all lung-related diagnoses easily.

REFERENCES

- [1] Haritha, D., Pranathi, M. K., & Reethika, M. (2020). COVID Detection from Chest X-rays with DeepLearning: CheXNet. 2020 5th International Conference on Computing, Communication and Security (ICCCS).
- [2] Awan, M. J., Bilal, M. H., Yasin, A., Nobanee, H., Khan, N. S., & Zain, A. M. (2021). Detection of COVID-19 in chest X-ray images: A big data enabled deep learning approach. *International journal of environmental research and public health*, 18(19), 10147.
- [3] Brunese, L., Mercaldo, F., Reginelli, A., & Santone, A. (2020). Explainable deep learning for pulmonary disease and Coronavirus COVID-19 detection from X-rays. *Computer Methods and Programs in Biomedicine*, 196(105608), 105608. <https://doi.org/10.1016/j.cmpb.2020.105608>
- [4] Gouda, W., Almurafeh, M., Humayun, M., & Jhanjhi, N. Z. (2022, February). Detection of COVID-19 Based on Chest X-rays Using Deep Learning. In *Healthcare* (Vol. 10, No. 2, p. 343). MDPI.
- [5] Hassantabar, S., Ahmadi, M., & Sharifi, A. (2020). Diagnosis and detection of infected tissue of COVID-19 patients based on lung x-ray image using convolutional neural network approaches. *Chaos, Solitons, and Fractals*, 140(110170), 110170. <https://doi.org/10.1016/j.chaos.2020.110170>
- [6] Phankokkruad, M. (2020, July). COVID-19 pneumonia detection in chest X-ray images using transfer learning of convolutional neural networks. In *Proceedings of the 3rd international conference on data science and information technology* (pp. 147-152).
- [7] Abraham, B., & Nair, M. S. (2020). Computer-aided detection of COVID-19 from X-ray images using multi-CNN and Bayesnet classifier. *Biocybernetics and Biomedical Engineering*, 40(4), 1436–1445. <https://doi.org/10.1016/j.bbe.2020.08.005>
- [8] Ausawalaithong, W., Thirach, A., Marukatat, S., & Wilaiprasitporn, T. (2018, November). Automatic lung cancer prediction from chest X-ray images using the deep learning approach. In *2018 11th Biomedical Engineering International Conference (BMEiCON)* (pp. 1-5). IEEE.
- [9] Amyar, A., Modzelewski, R., Li, H., & Ruan, S. (2020). Multi-task deep learning based CT imaging analysis for COVID-19 pneumonia: Classification and segmentation. *Computers in Biology and Medicine*, 126(104037), 104037. <https://doi.org/10.1016/j.combiomed.2020.104037>
- [10] Ibrahim, D. M., Elshennawy, N. M., & Sarhan, A. M. (2021). Deep-chest: Multi-classification deep learning model for diagnosing COVID-19, pneumonia, and lung cancer chest diseases. *Computers in biology and medicine*, 132, 104348.
- [11] Mahbub, M. K., Biswas, M., Gaur, L., Alenezi, F., & Santosh, K. C. (2022). Deep features to detect pulmonary abnormalities in chest X-rays due to infectious diseaseX: Covid-19, pneumonia, and tuberculosis. *Information Sciences*, 592, 389–401. <https://doi.org/10.1016/j.ins.2022.01.062>
- [12] Khan, E., Rehman, M. Z. U., Ahmed, F., Alfouzan, F. A., Alzahrani, N. M., & Ahmad, J. (2022). Chest X-ray classification for the detection of COVID-19 using deep learning techniques. *Sensors*, 22(3), 1211.

[13] Mehta, T., & Mehendale, N. (2021). Classification of X-ray images into COVID-19, pneumonia, and TB using cGAN and fine-tuned deep transfer learning models. *Research on Biomedical Engineering*, 37(4), 803-813.

[14] Yildirim, M., Eroğlu, O., Eroğlu, Y., Çinar, A., & Cengil, E. (2022). COVID-19 Detection on Chest X-ray Images with the Proposed Model Using Artificial Intelligence and Classifiers. *New Generation Computing*, 1-15.

IDENTIFICATION OF COVID-19, PNEUMONIA, LUNG CANCER & TB FROM CHEST X-RAY IMAGES: A DEEP TRANSFER LEARNING APPROACH

ORIGINALITY REPORT

22%
SIMILARITY INDEX

19%
INTERNET SOURCES

12%
PUBLICATIONS

13%
STUDENT PAPERS

PRIMARY SOURCES

1 dspace.daffodilvarsity.edu.bd:8080 **10%**
Internet Source

2 github.com **3%**
Internet Source

3 Masum Shah Junayed, Afsana Ahsan Jeny, Syeda Tanjila Atik, Nafis Neehal, Asif Karim, Sami Azam, Bharanidharan Shanmugam. "AcneNet - A Deep CNN Based Classification Approach for Acne Classes", 2019 12th International Conference on Information & Communication Technology and System (ICTS), 2019 **1%**
Publication

4 link.springer.com **1%**
Internet Source

5 Submitted to Daffodil International University **1%**
Student Paper

6 doctorpenguin.com
Internet Source